Science Press

ARTICLE

Deformation Behavior of TC4 Titanium Alloy Laser Welded Butt Joint Under Static Tensile Loading

Duan Aiqin,   Wang Zhensu,   Peng Huan,   Ma Xuyi

Science and Technology on Power Beam Process Laboratory, AVIC Manufacturing Technology Institute, Beijing 100024, China

Abstract: Static load tension is the most widely used mechanical properties test. In this paper, the influence of the laser welded joint on the deformation behavior of the specimen was revealed by comparing the thermal effects of TC4 base metal and joint specimen during tensile test through infrared thermograph method. The results show that for the joint and base metal specimens with the same tensile strength, there are many differences in the thermal effect, such as the beginning time of the physical yield phenomenon and the corresponding stresses, the temperature distribution and evolution process.

Key words: TC4 titanium alloy; laser welded joint; static tension; infrared thermograph method

Static load tensile test is the most widely used mechanical properties test for materials. It can reveal the basic mechanical behavior law of the material, and is also the basic test method for mechanical properties of materials[1].

Many related researches on the tensile mechanical properties of TC4 titanium alloy laser welded joint have been conducted by tensile test. For instance, Liang et al [2] showed that after laser welding of 1.8 mm thick TC4 titanium alloy sheets, the tensile strength and yield strength of the joints are significantly increased. During the tensile test, the deformation of the joint, the heat affected zone and the base metal are inconsistent, resulting in a significant decrease in the elongation of laser welded joint, only 58% of that of the base metal. Although the strength of the laser welded joint is quite different from that of the base metal, the yield strength ratio between them is consistently distributed between 0.91~0.92. Yang[3] showed that for TC4 titanium alloy laser welded joints, when the heat input is greater than 24 J/mm, the specimens are broken in the base metal, away from the joint center, and the joint elongation is about 67%~78%, and that when the heat input is less than 24 J/mm, the specimen is broken in the joint area, but the joint elongation is up to 87% of that of the base metal. Yang et al[4] showed that when TC4 titanium alloy sheet is annealed after laser welding, the tensile strength and elongation of the base metal are about 1086 MPa and 12.96%,

and those of the joint are about 1022 MPa and 10.94%, respectively. Dong et al [5] showed that the average tensile strength of TC4 titanium alloy laser welded joints is 1126.34 MPa, which is equivalent to that of the base metal, and the elongation is 11.12%, which is slightly lower than that of the base metal.

Although there are some differences in the results, generally speaking, the tensile strength and yield strength of TC4 titanium alloy laser welded joint are equivalent to those of the base metal, while the elongation is slightly lower than that of the base metal. The specimens may break in the base metal or joint area. The tensile test instrument can record the overall stress-strain curve of the specimen, giving macro-mechanical performance results of the engineering evaluation. But it is difficult to give detailed results of the performance of the special spot or area in the specimen during the loading process. These results are inadequate for research and evaluation of laser welded joint, as welded area is a small fraction of the specimen and has large changes in the structure. At present, with the development of infrared thermography, the accuracy and efficiency of temperature field measurement and recording are getting higher and higher. It can be applied to the tensile and fatigue test to study the temperature change across the whole specimen surface with the increase of load, and analysis of stress and strain evolution[6]. This method is of

important value for studying the mechanical properties and many other aspects of welded joint. Many studies have been carried out to detect the occurrence of damage and to investigate the fatigue and tensile process by infrared thermography method. For instance, Wang et al [7] investigated several thermal effects of polymer materials during the tensile process by infrared thermography. However, most studies about welded joint are concentrated on fatigue damage and fatigue life prediction[8-13]. In this paper, the influence of the joint on the deformation behavior was revealed by comparing the temperature evolution of TC4 base metal and laser welded joint specimen during the tensile process.

1 Experiment

In this paper, a 2 mm thick TC4 titanium alloy plate was fiber laser butt joint welded. Pre-weld specimens were routinely treated and cleaned, and welding process was according to the conventional welding requirements of titanium alloy using Ar gas for double-sided protection.

The tensile test specimens were designed in accordance with the relevant standards of static tensile test and requirements of infrared thermography system, as shown in Fig.1. The tensile specimens with no obvious defects were extracted from base plates and welded plates and tested at room temperature (loading rate was 3 mm/min) to analyze the joint performance. At the same time, a SC7000 IR camera was placed in front of the specimen to record the infrared thermal images of the tested part of specimen at a frequency of 50 Hz with resolution of 640×512 pixels. The ratio between specimen size and the image was about 0.1 mm per pixel. Before the test, thin mat black coatings were coated on the specimens to avoid reflections from the environment and to increase their emissivity, ensuring an accurate temperature measurement. All temperature data in this paper was not corrected for emissivity.
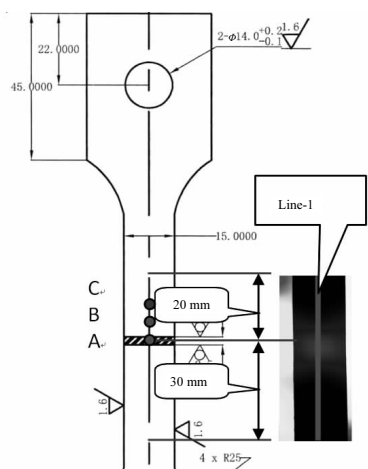

Fig.1 Geometry of the tensile test specimen, position of characteristic spots (A, B, C) and line-1

2 Result and Discussion

2.1 Conventional tensile test results

Tables 1 and 2 show the tensile properties of base metal and laser welded joint of TC4 titanium alloy. The results show that the tensile strength and yield strength of the joint are similar to those of base metal, and the dispersion of them is smaller. The difference in maximum P_{cd} (P_{cd}=crosshead displacement/60 mm) of the two specimens is slightly larger, and the average of joint specimens is about 92% of the base metal. In order to investigate the similarity and difference in the tensile process of the joint and the base metal, the base metal M-1 and the joint W-1 were selected as the detailed research objects. Fig.2 shows the stress-time curve of the specimen M-1 and W-1 recorded by the testing machine. It can be found that the two curves are very similar, and fracture of the joint specimen also occurs at base metal area (as shown in Fig.3). So it can be considered by the tensile test that the two specimens have the exactly same tensile performance and tensile process. Under this condition, through analyzing a series of infrared thermal images recorded by infrared thermograph, the deformation behavior of the two specimen will be further studied. In this paper, all tensile tests use the same uniform loading rate, and the loading time has a linear relationship with the P_{cd}. So in the following studies, the time axis will replace the crosshead displacement axis for synchronizing the infrared thermal image and the tensile test results.

2.2 Thermal effects of the specimens during the tensile process

The following studies are based on the results of the synchronization, which uses a unified time axis for tensile test

Table 1 Tensile test results of TC4 base metal and joints

Specimen	Tensile strength/MPa	Yield stress/MPa	Max P_{cd}/%	Sum of loading time/s
M-1	1046	899	10.3	126.43
M-2	1046	892	10.8	132.2
M-3	1036	894	10.3	126.35
W-1	1031	888	10.2	125.55
W-2	1044	906	9.39	116.05
W-3	1034	894	9.29	114.88

Table 2 Results based on infrared thermography for TC4 base metal and joints

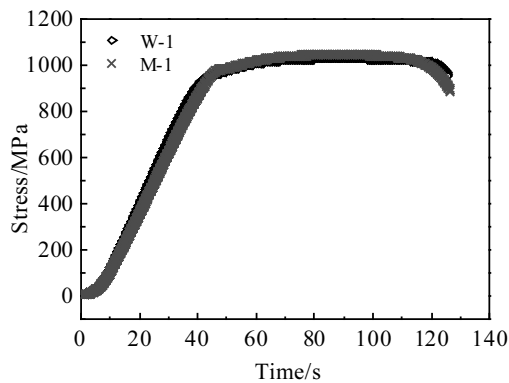| Specimen	Time of physical yield/s	Stress of physical yield/MPa	Physical yield position	Fracture location
M-1	45.6	971	Center	Center
M-2	46.06	976	Center	Center
M-3	44.52	946	Center	Center
W-1	38.98	895	Weld	Base metal
W-2	36.76	873	Weld	Base metal
W-3	37.06	868	Weld	Base metal

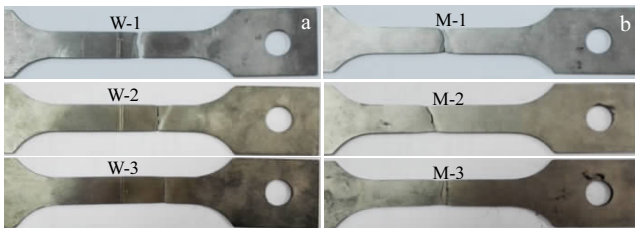Fig.2　Stress-time curve of joint W-1 and base metal M-1 specimens

Fig.3　Images of joint (a) and base metal (b) specimens after the tensile test

data and the infrared thermographic images. At the same time, for eliminating effects of the ambient temperature on the different specimens, the images were corrected according to the average value of the specimens before test.

Firstly, the center point spot-A of the specimen W-1 and M-1 is selected as the characteristic point, and the temperature evolution of the spot with the loading time is analyzed from the collected series of the images (as shown in Fig.4). The curves can be roughly divided into four stages according to the temperature characteristics: the temperature decrease stage (I), the rapid temperature increase stage (II), the temperature holding stage (III), and the temperature drop stage after
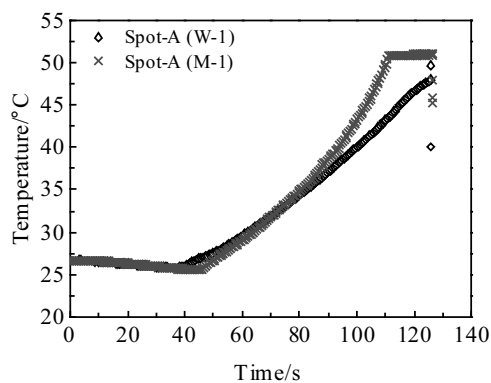
fracture (IV). Comparing the performance of specimen W-1 and M-1 in these four stages, the following findings can be found:

1) The temperature decrease stage (I). According to the thermal effect theory of materials during tensile process, the specimen is elastically deformed in this stage. And it can be found that the two curves are basically the same before the temperature rises, but the beginning time of this transition is quite different. The results of spot-A show that specimen W-1 starts to transform about 6 s earlier than M-1. It is known that the temperature rise indicates significant plastic deformation at that point. So the results reveal that in the early elastic deformation, there is no significant difference between the joint W-1 and base metal M-1 specimens, but at least for spot-A, the joint specimen undergoes an earlier plastic deformation. Form further analysis of the temperature of spot-A, B, C in W-1 (shown in Fig.5), it can be found that the curves of spot-A and spot-B at this stage are almost coincident. Although this specimen fractures at spot-C, its beginning time of the transition is delayed by about 3 s. The results indicate that the final fracture position of the joint specimen is not the same as the position where the plastic deformation occurs first.

2) The rapid temperature increase stage (II) and the temperature holding stage (III). These two stages belong to the plastic deformation stage. For the two type specimens, the curves of spot-A have obvious differences in these stages. Fig.4 shows that when the time<80 s, the curves are almost the same. But when time=80~110 s, the temperature rise rate of M-1 is significantly faster than that of W-1. When time>110 s, for M-1, the temperature holding stage (III) appears, but for W-1, the temperature at spot-A still linearly rises until the fracture, and there is no temperature holding stage (III), which is different from the base metal specimen. However, from Fig.5, it can be found that the W-1 at spot-C also has the temperature holding stage when time>100 s.

Fig.4　Temperature-loading time curves of spot-A in Fig.1 of the specimen W-1 and M-1
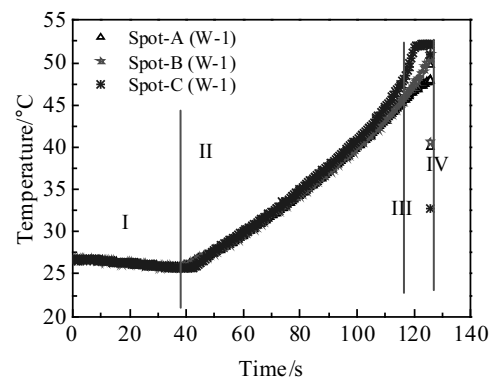

Fig.5　Temperature-loading time graph of spot-A, B and C in Fig.1 of the specimen W-1 (spot-A: joint center; spot-B: 4 mm from the center; spot-C: fracture position, 10 mm from the center)

3) The temperature drop stage after fracture (IV). In this stage, there is no obvious difference between W-1 and M-1 specimens. Both of them are instantaneous fracture and the highest temperatures have no apparently difference.

In summary, the temperature characteristics obtained from the thermographic images indicate that although the tensile strength, yield strength and the fracture time of the two type specimens are basically the same, there are differences between the two tensile processes. There are at least two apparent differences, which are the beginning time of the temperature from the decline to rise and the temperature rise rate. This means that even though the conventional static tensile property of the joint is the same as that of the base metal, the behavior of elastic and plastic deformation is quite different. In the following, these differences and the universal rule are further analyzed according to the series temperature field images and the temperature profile of line-1 (shown in Fig.1).

Material physical yield phenomenon is defined as[1]: for the forced specimen, the stress reaches a certain value, and the beginning of large-scale plastic deformation is called as yield. However, the conventional yield strength is a kind of engineering definition that is different from the physical yield phenomenon. In this paper, in order to study the deformation behavior of joints and base metal specimens in detail, the physical yield point of the specimen was defined. Based on the thermal effect theories of material elastic and plastic deformation, the time, which is needed to reach average temperature (the region: ±2 mm) of the specimen from the descending to rising, is defined as the physical yield point of the specimen, or the demarcation point between the elasticity and plasticity of the specimen. The region where the first transition begins to occur is defined as the location where the physical yield point occurs. It should be noted that the physical yield point defined in this paper is completely different from the conventional yield strength engineering definition, it is just the beginning time of physical yield phenomenon according to the thermal effects. Of course, corresponding stress and strain at the physical yield point can be obtained from the synchronized convention tensile test data.

According to this definition, the average temperature of the special area of the specimen W-1 and the M-1 was calculated. The results show that when time=38.98 s, the physical yield point of the W-1 appears at joint center, and the corresponding stress and P_{cd} are 895 MPa and 2.53%, respectively. When time=45.6 s, the M-1 has physical yield points at several areas, and the corresponding stress and P_{cd} are 971 MPa and 3.03%, respectively. These results reveal that although the yield strengths of the two specimens are almost the same, the time of physical yield point of W-1 is 6.62 s earlier than that of M-1, and the stress and P_{cd} differences are 76 MPa and 0.5%, respectively. So, it can be concluded at least that the presence of the joint has a great effect on the beginning time of physical yield phenomenon and corresponding stress and P_{cd}.

In order to facilitate the comparison, a new synchronizing time t_{e-p} was used to reset the temperature field image of the specimen, that is, the time at which the physical yield phenomenon occurs at the same time was assumed to be t_{e-p}=0 s, and then the temperature field images at this time were compared and analyzed. For the W-1, the temperature field images at t_{e-p}=−6, −3, 0, ..., 85, 86. 58 s was selected for detailed studies (shown in Fig.6a), where t_{e-p}=−6, −3 s, showing the elastic deformation stage characteristics. The temperature field images of the M-1 are selected at the same time for comparison and analysis (shown in Fig.6b). It can be clearly seen that even if the mechanical properties of the two type specimens are similar, the presence of joint has a quite effect on the elastic and plastic deformation behavior during tensile process. Fig.7 shows the line-1 temperature profile of the two specimens at the same t_{e-p}. Results show that:

1) When t_{e-p}=−6 s (W-1: 757 MPa, 2.08%; M-1: 858 MPa, 2.58%), the specimens W-1 and M-1 are in elastic deformation stage, basically similar, and evenly distributed. The line-1 temperature average is 25.82 and 25.65 °C, and the standard-deviation (Std-Dev) is 0.06 and 0.04 °C, respectively.

2) When t_{e-p}=−3 s (W-1: 831 MPa, 2.31%; M-1: 922 MPa, 2.81%), the W-1 and M-1 are still in the elastic deformation stage; the line-1 temperature average is 25.73 and 25.58 °C, the Std-Dev is 0.07 and 0.05 °C, respectively, and the data dispersing slightly increases. The images and the profiles are similar to those at t_{e-p}=−6 s. The temperatures of line-1 are uniformly distributed and the average decreases, meaning an obvious thermo-elastic effect.

3) When t_{e-p}=0 s (W-1: 895 MPa, 2.53%; M-1: 971 MPa, 3.03%), the local physical yield phenomenon of W-1 and M-1 begins to appear. For the W-1, there is an apparent temperature rise in the weld and its vicinity, and the line-1 profile changes from the previous uniform distribution to the Gaussian distribution, while the M-1 keeps uniform distribution. The temperature average is 25.71 and 25.63 °C, the Std-Dev is 0.13 and 0.04 °C. These results show that at the beginning of the physical yield phenomena, the presence of the weld leads to an increase in the deformation homogeneity, and the plastic deformation mainly concentrates in the weld. From Fig.7, it can be clearly seen that across ±10 mm region, the temperature of the W-1 is still in a downward trend, indicating that these parts are still in the elastic deformation state. This phenomenon may be because at this time the stress of 895 MPa is not able to lead to the plastic deformation of base metal areas, just taking in the weld. This conclusion can be confirmed by the result of the base metal specimen M-1, whose physical yield stress is 971 MPa.

4) When t_{e-p}=3 s (W-1: 942 MPa, 2.76%; M-1: 982 MPa, 3.27%), the temperature of the W-1 specimen still keeps the Gaussian distribution and the temperature of the weld area rises apparently, and that of the rest areas begins to rise.

t_{e-p}: -6 s	-3 s	0 s	3 s	6 s	9 s	12 s	15 s	a

Stress/MPa:	757	831	895	941	958	969	981	992
P_{cd}/%:	2.08	2.31	2.53	2.76	3	3.26	3.53	3.8

t_{e-p}: 30 s	40 s	50 s	60 s	70 s	80 s	85 s	86.6 s

Stress/MPa:	1020	1030	1030	1030	1020	1010	988
P_{cd}/%:	5.15	6.05	9.95	7.85	8.75	9.65	10.1

t_{e-p}: -6 s	-3 s	0 s	3 s	6 s	9 s	12 s	15 s	b

Stress/MPa:	858	922	971	982	990	1000	1010	1020
P_{cd}/%:	2.58	2.81	3.03	3.27	3.53	3.81	4.07	4.35

t_{e-p}: 30 s	40 s	50 s	60 s	70 s	75 s	80 s	80.84 s

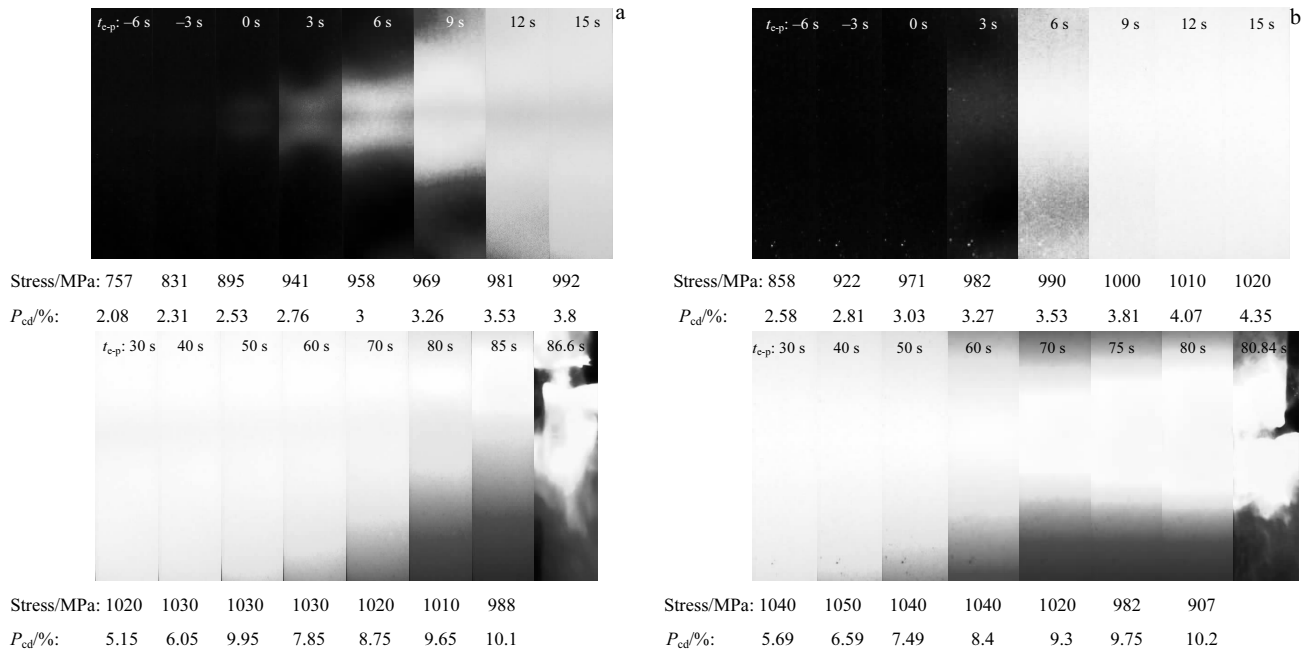| Stress/MPa:	1040	1050	1040	1040	1020	982	907
P_{cd}/%:	5.69	6.59	7.49	8.4	9.3	9.75	10.2

Fig.6   Temperature field images of specimens W-1 (a) and M-1 (b)

These indicate that at this time, although the plastic deformation of the weld area is still large, it occurs in the entire test section of the specimen, different from at t_{e-p}=0 s, at which it only occurs in the weld. The line-1 temperature profile of the M-1 is "W" type, the average is 26.25 °C, higher than 25.89 °C of the W-1 specimen, but the max value of 26.41 °C is still lower than 26.57 °C of the W-1 specimen. The Std-Dev is 0.28 and 0.07 °C; compared with the results of 0.13 and 0.04 °C at t_{e-p}=0 s, it can be known that although the un-uniformity of plastic deformation of both specimen increases, the difference of the joint specimen is particularly large.

5) When t_{e-p}=6 s (W-1: 958 MPa, 3%; M-1: 990 MPa, 3.53%), for the specimen M-1, the most obvious feature is that the average and max temperature values are larger than those of specimen W-1, and uniformity remains (Std-Dev is 0.07 °C). But for the specimen W-1, the Std-Dev is 0.3 °C; the growth rate becomes smaller obviously than before, and double peaks of temperature begin to occur around the weld area, which is low in the weld center; both sides of the heat affected area are slightly higher, and the rest area continues to rise.

6) When t_{e-p}=9 s (W-1: 3.26%; M-1: 3.81%), for the specimen W-1, the temperature rise of the weld area slows down and that of the rest area rises rapidly, and more obvious bimodal phenomenon appears around the weld. The average temperature increases to 27.12 °C, but the Std-Dev decreases to 0.2 °C, showing a leveling trend. For the M-1, the image clearly shows that the temperature distribution throughout the region is uniform and the line-1 profile is still almost uniformly and linearly distributed. But the overall temperature

rises to the average of 27.72 °C, and the Std-Dev has a slight decrease from 0.07 to 0.06 °C.

7) When t_{e-p}=12 s (W-1: 3.53%; M-1:4.07%), for the W-1, the weld area has a more obvious temperature concave trend, although the double peak still exists, obviously shifting to both sides of the base metal (peak at ± 8 mm or so). At this time, the average temperature rises to 27.81 °C and the Std-Dev decreases to 0.15 °C, which means the obvious leveling trend. The temperature of the weld center is 27.81 °C, but the peak is 28.08 °C. If the heat conduction effect is taken into account, the weld center temperature must be lower, and the double peak should be higher, which means that the plastic deformation of the weld area is weakened, while that of the base metal area is strengthened. However, the image of the M-1 shows that the temperature distribution in the whole area keeps uniform, but the line-1 profile shows that arc temperature distribution of the specimen center has the highest point; the overall temperature rises, the average is 28.41 °C, and the Std-Dev is 0.07 °C.

8) When t_{e-p}=15~60 s (W-1: 3.8%~7.85%; M-1: 4.35%~8.4%), for the specimen W-1, it maintains the trend of temperature evolution at t_{e-p}=12 s, and the weld area keeps the temperature downward trend, but the temperature difference decreases gradually with time. The bimodal phenomenon gradually disappears, and the temperature of the base metal on the both sides of the weld tends to be smooth, which indicates that the plastic deformation is gradually uniform throughout the test section. The images intuitively show these results, except for the surrounding of the weld, which is in deep color and becomes unobvious with the increase of time, and the color
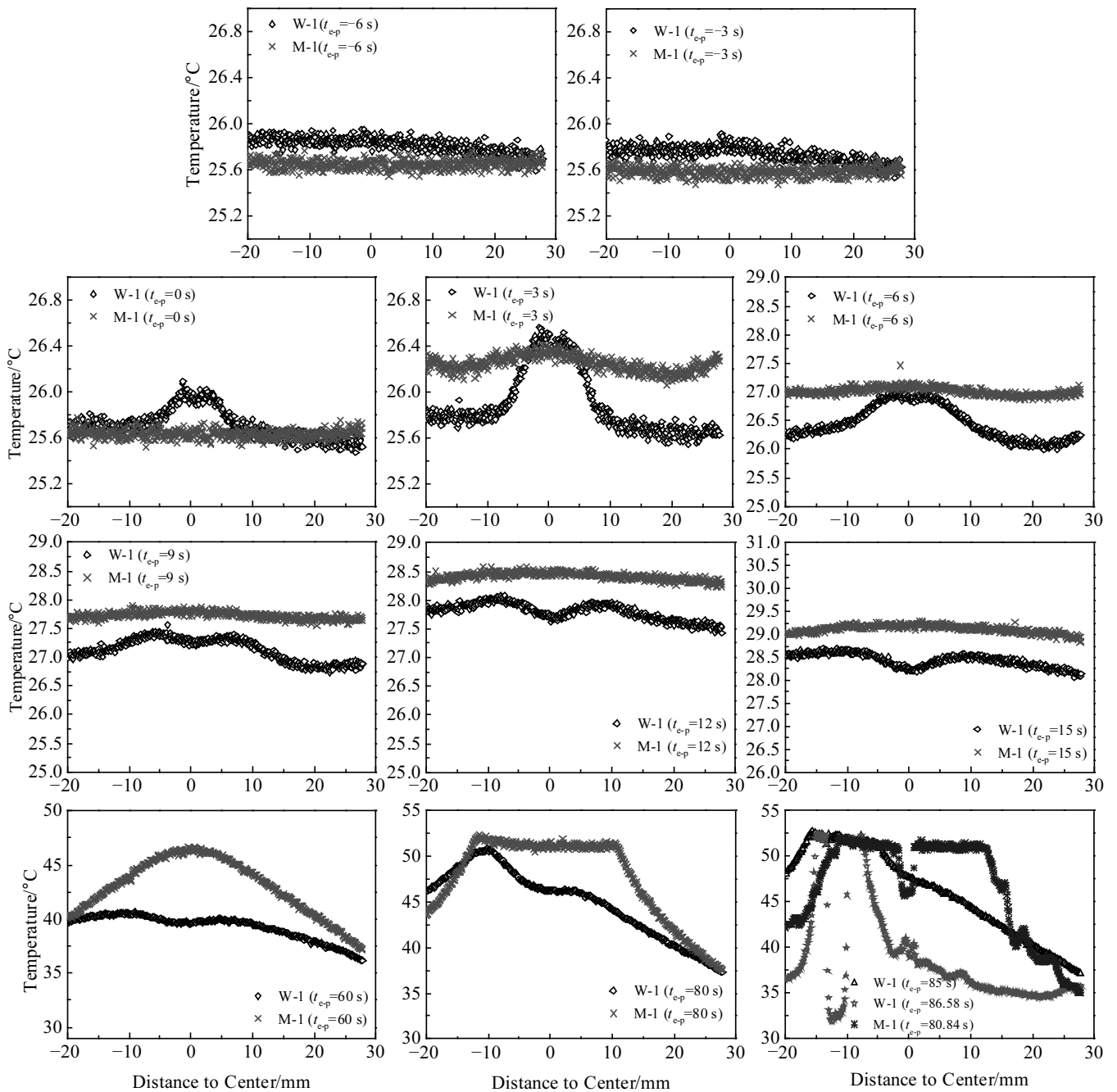
Fig.7   Comparison of line-1 temperature profiles of the specimen W-1 and M-1 at different time

of the rest areas tends to be uniform. For the base metal specimen M-1, it also maintains the arc temperature distribution trend with the highest point in the specimen center, and this trend gradually increases with time, while the overall temperature rises, which is higher than that of the specimenW-1 at the same time.

9) For t_{e-p}=60~80 s (W-1: 7.85%~9.65%; M-1: 8.4%~10.2%), the specimen W-1 starts to show a new temperature peak at about d=−10 mm, which increases with the loading time. Apparently necking phenomenon appears at this position,

and it is the final fracture position of the specimen. During this process, the concave of the weld area in the line-1 profile becomes not obvious, and the temperature rise on the one side becomes slower than that on the other side, which indicates that the plastic deformation begins to focus on the necking area. This phenomenon can be seen more clearly in the images, where high temperature areas are concentrated on the top of images. For the specimen M-1, the images show that the high temperature area is concentrated in the middle of the specimen. And the profile shows that the temperature distribution

characteristic changes. The max temperature is maintained at about 52.14 °C in a certain area, forming a uniform distribution segment, and the length increases from ±8 mm to ±12 mm with loading time, while the rest shows a linearly downward trend with the distance from the center of the specimen. Taking the heat transfer mechanism into account, it can be inferred that the plastic deformation occurs only in this uniform distribution segment, and from the images it can be found that in this section, the necking phenomenon is gradually obvious, until the fracture occurs in this necking area.

10) When t_{e-p}=80.84 s, fracture occurs in the middle position of M-1, while at t_{e-p}=86.58 s, the joint specimen W-1 fractures in the base metal area. For the two specimens, there is an obvious necking phenomenon at the fracture area before the fracture, and no obvious difference in the fracture.

2.3 Repeatability analysis of temperature field evolution and deformation behavior

From the above results of the specimen W-1 and M-1, it can be found that even if the tensile mechanical properties are substantially equivalent, the presence of joint still has a large effect on the deformation behavior, including the beginning time, location and stress of the physical yield point, plastic deformation evolution rule at different locations. In order to verify the repeatability of these results, the same analysis was performed on other four specimens.

Fig.8 and Fig.9 show the images and line-1 temperature profile of the joint specimen W-2 and W-3 and the base metal specimen M-2 and M-3, respectively. Combining the relevant results in Tables 1 and 2, it can be concluded that the rules are basically the same as those of the specimen W-1 and M-1:

1) The physical yield of W-2 and W-3 also occurs first at the weld but fracture occurs at the base metal. Compared with W-1, the tensile strength, yield strength of the W-2 and W-3 are basically the same, but the maximum P_{cd} and fracture time are slightly lowered by about 9%. The time and stresses of the physical yield point are 36.76 and 37.07 s, and 873 and 868 MPa, respectively, which are slightly smaller than 906 and 894 MPa of the convention yield strength. But the physical yield of the base metal specimen M-2 and M-3 is substantially the same as that of M-1.

2) After the physical yield occurs, the W-2 and W-3 have almost the same evolution as W-1. The temperature profiles change from the previous uniform distribution to the Gaussian distribution, indicating that the presence of the weld causes the un-uniform deformation increase, and the plastic deformation at this time is mainly concentrated in the weld area. When t_{e-p}=3 s, temperatures of the joint specimens are more obvious Gaussian distribution, and temperature in the weld area rises significantly. When t_{e-p}=12 s, obvious bimodal phenomenon appears at the center of the weld areas, and the temperature rise around the weld slows down, while in another areas, the temperature begins to rapidly rise. Then double peaks shift on both sides of the weld and gradually disappear, in which the temperature flattening phenomenon is obvious. At t_{e-p}=50~70 s, a new peak occurs upside the specimens, and then the concave of the weld areas in the curve becomes not obvious, and the temperature rise on the one side becomes slower than that on the other side, which indicates that the plastic deformation is focused on the necking position until fracture occurs at that position. The M-2 and M-3 also show the same temperature
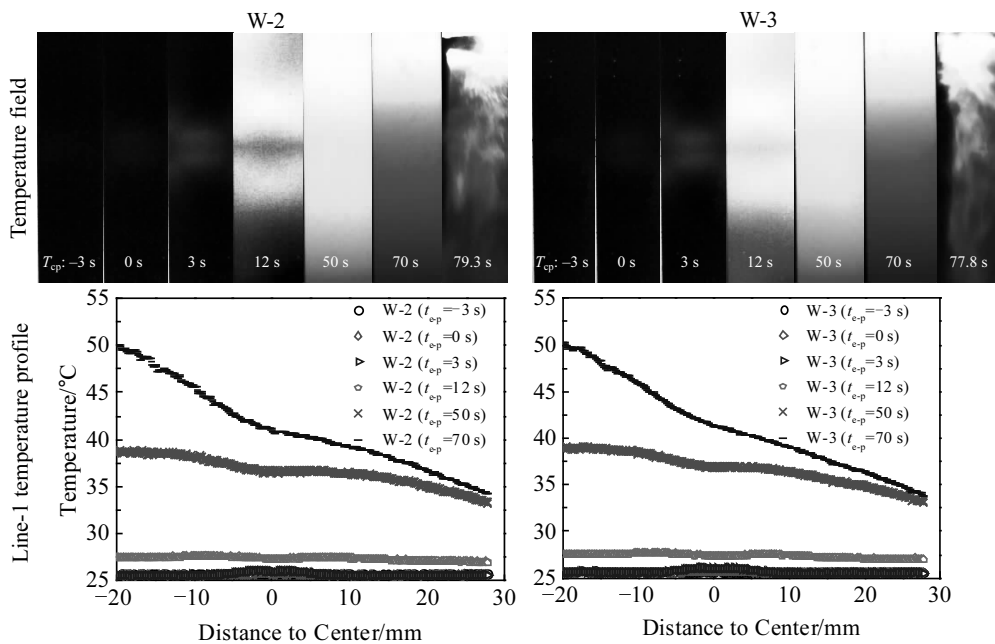

Fig.8   Joint specimen W-2 and W-3 temperature field images and line-1 temperature profile at different time
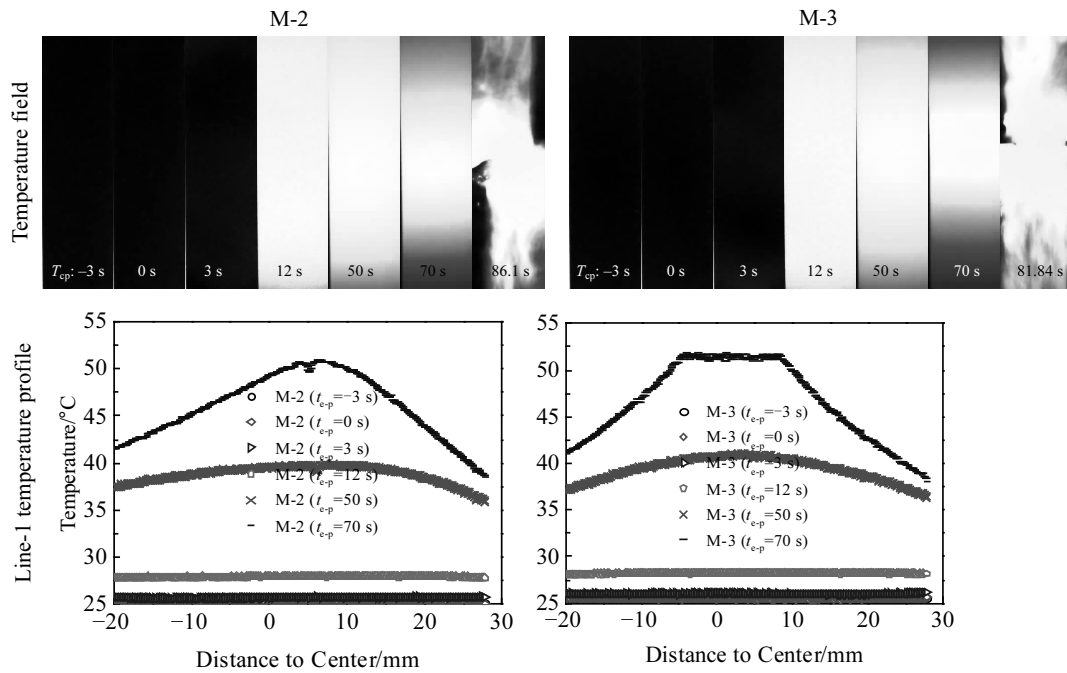
Fig.9　Specimen M-2 and M-3 temperature field images and line-1 temperature profile at different times

evolution rule as the M-1.

In view of the above analysis, for the three joint specimens without obvious defects and the three base metal specimens, the thermal effect characteristics and plastic deformation evolution rule have good repeatability.

3　Conclusions

1) The temperature evolution of the characteristic spot of specimens with loading time can be divided into four stages, namely, the temperature decrease stage, the rapid temperature increase stage, the temperature holding stage and the temperature drop stage after fracture, indicating that the specimen undergoes elastic deformation, plastic deformation, plastic deformation of the necking phenomenon, and fracture.

2) Although the joint and base metal specimens have basically the same tensile strength, the yield strength and the loading time, there are many differences in the thermal effect between them, such as the beginning time and the location of the physical yield and corresponding stresses. After the physical yield, the basic trend of the two type specimens is that the temperature increases with the loading time. But its temperature distribution and evolution process are very different, indicating that the joint has a greater effect on the plastic deformation of the specimen.

References

1　Liu Ruitang, Liu Jinyun. *Mechanical Properties of Metal Materials*[M]. Harbin: Harbin Institute of Technology Press, 2015: 3

2　Liang Chunlei, Li Xiaoyan, Li Shuigong *et al*. *Materials Engineering*[J], 2006, 4: 48 (in Chinese)

3　Yang Jing, Cheng Donghai, Huang Jihua *et al*. *Rare Metal Materials and Engineering*[J], 2009, 38(2): 259 (in Chinese)

4　Yang Wulin, Yang Xiaohua, Li Xiaoyan. *Materials Engineering*[J], 2012, 33(6): 80 (in Chinese)

5　Dong Zhijun, Lu Tao, Lei Zhenglong *et al*. *Space Manufacturing Technology*[J], 2013, 1: 27 (in Chinese)

6　Xu Bingye. *Application of Elastoplastic Mechanics*[M]. Beijing: Tsinghua University Press, 1995: 10

7　Wang Meng. *Thesis for Doctorate*[D]. Shanghai: Dong Hua University, 2012 (in Chinese)

8　Frank P, British Kruppler. *Heat Transfer and Mass Transfer Basic Principles*[M]. Beijing: Chemical Industry Press, 2007: 58

9　Zhang H X, Wu G H, Yan Z F *et al*. *Materials and Design*[J], 2014, 55: 785

10　Liu Xiaoqing, Zhang Hongxia, Yan Zhifeng *et al*. *Theoretical and Applied Fracture Mechanics*[J], 2013, 67-68: 46

11　Liu Jing, Gao Xiaolong, Zhang Linjie *et al*. *Jmepeg*[J], 2014, 23: 2965

12　Thomas Ummenhofer, Justus Medgenberg. *International Journal of Fatigue*[J], 2009, 31: 130

13　Thomson W. *Mathematical and Physical Papers*[M]. London: Focal Press, 1990

TC4 钛合金激光焊对接接头静力拉伸载荷下的变形行为特征

段爱琴，王振苏，彭　欢，马旭颐

(中国航空制造技术研究院　高能束流加工技术重点实验室，北京　100024)

摘　要：静载拉伸试验是最基本的、应用最广的材料力学性能试验。通过对静力拉伸载荷下 TC4 母材和激光焊缝接头试样红外热像的记录和温度场变化特征的对比分析，揭示激光焊缝的存在对于试样受力变形行为的影响规律。研究结果表明：宏观抗拉强度、屈服强度以及断裂时间都基本相同的焊缝和母材试样，其红外结果存在相同点，同时也存在明显的差异性。首先，开始出现物理屈服现象的时间以及对应的应力有差异；焊缝和母材试样在物理屈服发生后，其温度分布及演变规律具有很大的差异性，表明了焊缝的存在对试样的塑性变形规律具有较大的影响。

关键词：TC4 钛合金；激光焊接接头；静力拉伸；红外热像方法

作者简介：段爱琴，女，1966 年生，博士，研究员，中国航空制造技术研究院高能束流加工技术重点实验室，北京　100024，电话：010-85701428，E-mail: 13611384073@163.com